Quantifying Neuronal Information Flow in Response to Frequency and Intensity Changes in the Auditory Cortex

Ketan Mehta*, Jörg Kliewer†, Antje Ihlefeld‡
*Krasnow Institute for Advanced Study, George Mason University, Fairfax, VA 22030
†Helen and John C. Hartmann Dept. of Electrical and Computer Engineering
New Jersey Institute of Technology, Newark, NJ 07102
‡Dept. of Biomedical Engineering, New Jersey Institute of Technology, Newark, NJ 07102

***Abstract*—Studies increasingly show that behavioral relevance alters the population representation of sensory stimuli in the sensory cortices. However, the mechanisms underlying this behavior are incompletely understood. Here, we record neuronal responses in the auditory cortex while a highly trained, awake, normal-hearing gerbil listens passively to target tones of high versus low behavioral relevance. Using an information theoretic framework, we model the overall transmission chain from acoustic input stimulus to recorded cortical response as a communication channel. To quantify how much information core auditory cortex carries about high versus low relevance sound, we then compute the mutual information of the multi-unit neuronal responses. Results show that the output over the stimulus-to-response channel can be modeled as a Poisson mixture. We derive a closed-form fast approximation for the entropy of a mixture of univariate Poisson random variables. A purely rate-code based model reveals reduced information transfer for high relevance compared to low relevance tones, hinting that changes in temporal discharge pattern may encode behavioral relevance.**

I. Introduction

When sound reaches the ears, neurons throughout the entire auditory neuraxis, from auditory nerve to auditory cortex, encode this sensory information by transmitting information via electrical pulses, called spikes. In addition to sensory-evoked responses, these neurons also transmit non-sensory driven information, sometimes referred to as internal noise [1]. It is then of considerable interest to know how much information about the stimulus is actually contained in these neuronal spike responses [2], [3]. An extensive literature successfully applies the concepts of information theory to quantify neuronal information transfer [3]–[6] in response to stimulus for visual [6], auditory [7], [8], somatosensory [9], [10], or olfactory [11] neurons. Here we are interested to determine how well a Poisson model can describe neuronal responses in auditory cortex. Using this model we characterize the loss in mutual information from acoustic stimulus to neuronal response by providing an efficient way to compute mutual information, thus bypassing the need to directly estimate the corresponding distributions.

Work supported by NIH-NIDCD (R03 DC014008 to AI).

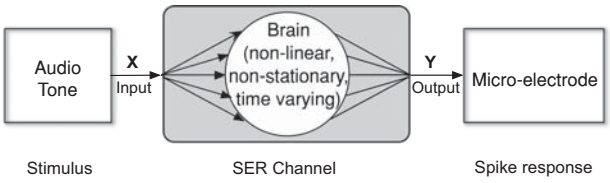

Fig. 1: Sound evoked response (SER) channel.

Specifically, we present a novel information theoretic framework to model the overall transmission chain from stimulus presentation to recorded cortical neuronal discharge as a communication channel. In the particular example tested here, the input to this communication channel is an acoustical signal, specifically, a pure tone with known frequency and intensity, and the output is the neuronal spike activity recorded in response to the stimulus via chronically implanted microelectrodes in the core auditory cortex. We refer to this communication channel as the sound evoked response (SER) channel and consider it equivalent to a non-linear, time-varying, point-to-point communication channel with memory, as shown in Fig. 1. We then characterize the SER channel of a Mongolian gerbil trained to detect 1 kHz tones via its associated mutual information.

Previous work suggests that the auditory cortex changes its response properties depending on the behavioral significance of selected sound [12]–[14]. However, scant computational tools exist for directly characterizing how much information about the behavioral relevance of sound is contained in the spiking rate of neurons in auditory cortex [15], [16]. In general, neurons in the auditory pathway encode sound features both through firing rate and spike timing [17]–[19]. We show in the following work that the sound-evoked responses of core auditory cortex neurons can be modeled as a Poisson mixture model [20], [21]. We then calculate the mutual information (MI) over the SER channel to determine how separable the spike rate responses are for pure tone stimuli of one behaviorally relevant and four behaviorally irrelevant frequencies, respectively. Our hypothesis is that the MI of the SER channel changes in response to behaviorally relevant sound. This

means that here, we expect to see a change in MI over the SER channel for a 1 kHz stimulus as compared to the other behaviorally irrelevant frequencies. Across the population of neurons, we also expect to see an increase in firing rate with increasing sound intensity. Therefore as verification of our model, we expect to see higher MI for louder as compared to softer sound pressure levels (SPLs).

Further, while the Poisson mixture is an often occurring model in the literature, there exists no closed-form solution to calculate its entropy [22], [23]. As a major contribution of this work we derive a closed-form approximation for the entropy of a mixed pair of univariate Poisson random variables. The presented analytical expression reduces the complexity from $\mathcal{O}(n^2 \log n)$ required for a numerical calculation to a finite constant complexity $\mathcal{O}(1)$, thus significantly speeding up the computations of the SER channel MI in our experiment.

II. Experiment Design and Method

All procedures were in accordance with the guidelines and rules of the Institutional Animal Care and Use Committee of New York University. Here, we tested one Mongolian gerbil *(Meriones unguiculatus)*, an animal with excellent human-like low frequency hearing, for which perception, neurophysiology and synaptic properties are well characterized [24], [25]. The trained, awake gerbil listened passively to pure tones of high versus low behavioral relevance while a multi-channel chronically implanted micro-electrode array (Neuronexus, A4x4-4mm-200-200-1250-H16_21 mm) recorded multi-unit neuronal spike activity in left core auditory cortex. The neuronal data was simultaneously recorded via seven electrodes at a sampling rate of 24 kHz (using methods for electrode implantation similar to [26]).

Prior to implantation, through positive reinforcement, the animal had been trained extensively to hear out 1 kHz target tones (see details in [27]). Thus, tones with a frequency of 1 kHz were of high behavioral relevance to this animal. In contrast, tones at four other frequencies (0.5, 2, 4, 8 kHz) were never encountered by the animal during prior training and testing and were thus of low behavioral relevance. Neuronal activity was recorded in response to high versus low behavioral relevance tones at four sound intensities (23, 33, 43, 53 dB SPL). As a control, non-auditory evoked neuronal activity was also recorded in silence. Each high and low relevance tone was presented for a duration of 1 second with a 10ms rise/fall. Data was collected over a total of 18 sessions, with 10 repetitions of each frequency-intensity combination per session.

A. Spike Detection

In order to detect spikes we first bandpass filter the raw data between 300-6000 Hz. An automatic threshold detector is then used to determine the height (amplitude) of the action potential and generate a pulse whenever the measured voltage crosses a set threshold.

Let the voltage amplitude of the filtered signal be denoted by random variable Z, which is considered to be a mixture of the spike amplitude component S_A, and a noise component N (with zero mean) [28]. Since the probability of spiking $p(s)$ is in fact very small (see Sec. II.B for details), the spike component in the signal is relatively sparse to the background noise activity. The median absolute deviation of the signal is therefore relatively unaffected by the spike component, i.e., median($|Z|$) $\approx$ median($|N|$). Further, we assume N to be Gaussian, and the detection threshold is estimated based on the median absolute deviation of the signal as [29],

$$\text{threshold} = c \cdot \frac{\text{median}(|Z|)}{0.6745}, \tag{1}$$

where c is a constant chosen between 3 and 5.

B. Probability distribution of the output spike sequence

With our model here we implicitly assume that the firing rate of the neuron contains information about the input stimulus, and that the underlying instantaneous firing rate r is constant over the time interval during which the stimulus remains fixed. We divide the total time T into M bins, each of duration $\Delta t = T/M$, where Δt is a small enough time interval such that there is no more than one spike in any one bin. The probability of a single spike occurring in one specific bin is then

$$p(s) = P\{\text{one spike in } \Delta t\} = r\Delta t. \tag{2}$$

Therefore, the probability of n spikes in M bins can be represented using a binomial distribution

$$P\{n \text{ spikes in } T\} = \binom{M}{n} (r\Delta t)^n (1 - r\Delta t)^{M-n}. \tag{3}$$

It can be shown that for small values of $p(s)$ and large values of M, the binomial distribution can be approximated by a Poisson distribution [30]. Therefore, the probability of n spikes in a time interval T can be expressed as a Poisson random variable N_λ with corresponding probability distribution

$$p(n;\lambda) = \frac{(Mr\Delta t)^n}{n!} e^{-Mr\Delta t} = \frac{(rT)^n}{n!} e^{-rT}, \tag{4}$$

where the mean spike rate, $rT = \lambda$, is the average number of spikes in a time interval of length T.

In this work, we used a time window of $T = 500$ ms beginning 100 ms after stimulus onset, and Δt to be 40 samples (approx. 2 ms). The spike rate λ was then determined using an estimator that minimizes the L_1 distance between the fitted Poisson distribution and the recorded spike sequence.

III. Information Theoretic Analysis of the SER Channel

We begin the information theoretic analysis by defining the input and output random variables of the SER channel. The input random variable X of the SER channel is uniformly distributed over a set of class indices $\mathcal{X}$ which describe the intensity and frequency of the stimulus auditory tone at any given time interval. For analytical tractability we choose here a binary input scheme for X. Also from a subjective viewpoint, a binary choice of input between a tone versus silence has the largest likelihood of having a prominent difference between

the evoked response for these two stimuli. Since all tones are equally likely and presented for an equal duration of time, let X be an equiprobable Bernoulli random variable

$$X = \begin{cases} x_1, & \text{input stimulus is tone+intensity combination} \\ x_2, & \text{input stimulus is silence}, \end{cases} \quad (5)$$

such that $p(x_1) = p(x_2) = 1/2$.

The output Y of the channel is given by the firing rate of the neuronal spike response, as recorded by the electrode. According to (4) then, the conditional distribution corresponding to the output of each electrode converges to a Poisson distribution

$$p(y|x_i) = p(n;\lambda_i) = e^{-\lambda_i}\frac{\lambda_i^n}{n!}, \quad i = 1, 2. \quad (6)$$

The conditional entropy $H(Y|X)$ is then given by

$$\begin{aligned} H(Y|X) &= -\sum_{x\in\mathcal{X}} p(x) \sum_{y\in\mathcal{Y}} p(y|x)\log p(y|x) && (7)\\ &= -\frac{1}{2}\sum_{n}\Big\{p(n;\lambda_1)\log p(n;\lambda_1) + \\ &\qquad\qquad p(n;\lambda_2)\log p(n;\lambda_2)\Big\} && (8)\\ &= \frac{1}{2}H(N_{\lambda_1}) + \frac{1}{2}H(N_{\lambda_2}) \text{ bits}, && (9) \end{aligned}$$

where $H(N_{\lambda_1})$ and $H(N_{\lambda_2})$ are the entropies of the Poisson distributions $p(n;\lambda_1)$ and $p(n;\lambda_2)$, respectively. In this work, we use $\log(\cdot)$ to denote logarithm to the base 2, while $\ln(\cdot)$ is the natural logarithm.

Using the law of total probability we can write $p(y)$ as

$$p(y) = \sum_{x\in X} p(y|x)p(x) = \frac{1}{2}\Big(p(n;\lambda_1) + p(n;\lambda_2)\Big). \quad (10)$$

The distribution $p(y)$ is therefore a mixture distribution of univariate Poisson distributions. Defining

$$\Phi(\lambda_1, \lambda_2, n) \triangleq \log p(y), \quad (11)$$

the entropy of Y is given by

$$H(Y) = -\sum_{n}\frac{1}{2}\Big(p(n;\lambda_1) + p(n;\lambda_2)\Big)\cdot\Phi(\lambda_1,\lambda_2,n). \quad (12)$$

A. Entropy of a univariate Poisson mixture

The entropy of a Poisson mixture model in (12) is an open problem in the literature. The expression for the entropy of the Poisson mixture consists of a summation over a logarithm of a sum of exponential and factorial functions which makes it difficult to formulate a general closed-form analytical solution. In the absence of an analytical solution, the complexity to numerically calculate a function of factorial and exponential terms ($f(n!, \lambda^n)$) is of the order $\mathcal{O}(n^2 \log n)$ [31]. Since the summation in the expression for entropy is computed over all n ranging from zero to infinity, this becomes a significant drawback when data from multiple trial sessions need to be processed in succession. Alternatively, we present here an approximation for the entropy of the univariate Poisson mixture. Further, we use the entropy approximation to provide a simple and elegant analytical expression for the fast estimation of the MI over the SER channel, drastically reducing the complexity.

Given any two given positive scalar values a and b the logarithm of their sum can alternatively be expressed using the Jacobian logarithm as

$$\log(a+b) = \max(\log a, \log b) + \log\left(1+\frac{\min(a,b)}{\max(a,b)}\right). \quad (13)$$

For a given particular value of $n = n_0$, we can use (13) to rewrite (11) as

$$\begin{aligned} \Phi(\lambda_1,\lambda_2,n_0) = \max(\log p(n_0;\lambda_1), \log p(n_0;\lambda_2)) - 1 \\ + \log\Big(1+\frac{\min(p(n_0;\lambda_1), p(n_0;\lambda_2))}{\max(p(n_0;\lambda_1), p(n_0;\lambda_2))}\Big). \end{aligned} \quad (14)$$

Further, given n_0, let us define $\lambda'_{n_0}, \lambda''_{n_0}$ such that

$$\lambda'_{n_0} \triangleq \underset{\lambda=\{\lambda_1,\lambda_2\}}{\arg\min}\left\{e^{-\lambda}\frac{\lambda^{n_0}}{n_0!}\right\}, \quad \lambda''_{n_0} \triangleq \underset{\lambda=\{\lambda_1,\lambda_2\}}{\arg\max}\left\{e^{-\lambda}\frac{\lambda^{n_0}}{n_0!}\right\}. \quad (15)$$

For simplicity, we write $\lambda' = \lambda'_{n_0}$, and $\lambda'' = \lambda''_{n_0}$. Now using (15) along with (6) we have

$$\frac{\min(p(n_0;\lambda_1), p(n_0;\lambda_2))}{\max(p(n_0;\lambda_1), p(n_0;\lambda_2))} = \left(\frac{\lambda'}{\lambda''}\right)^{n_0}\cdot e^{\lambda''-\lambda'} \le 1. \quad (16)$$

Solving for n_0 in (16)

$$n_0 \le \frac{\lambda'-\lambda''}{\ln\lambda' - \ln\lambda''}. \quad (17)$$

Therefore,

$$\begin{aligned} \Phi(\lambda_1,\lambda_2,n_0) = \max(\log p(n_0;\lambda_1), \log p(n_0;\lambda_2)) - 1 \\ + \log\Big(1+\Big(\frac{\lambda'}{\lambda''}\Big)^{n_0}\cdot e^{\lambda''-\lambda'}\Big). \end{aligned} \quad (18)$$

Let us also define $\lambda_{\max} \triangleq \max(\lambda_1,\lambda_2)$, $\lambda_{\min} \triangleq \min(\lambda_1,\lambda_2)$. We then use the following set of approximations:

$$\begin{aligned} &\log\Big(1+\Big(\frac{\lambda'}{\lambda''}\Big)^{n_0}\cdot e^{\lambda''-\lambda'}\Big) \approx \log\Big(1+\Big(\frac{\lambda_{\min}}{\lambda_{\max}}\Big)^{n_0}\Big) && (19)\\ &\le \log\Big(1+\Big(\frac{\lambda_{\min}}{\lambda_{\max}}\Big)^{\frac{\lambda'-\lambda''}{\ln\lambda'-\ln\lambda''}}\Big) && (20)\\ &\approx \log\Big(1+\Big(\frac{\lambda_{\min}}{\lambda_{\max}}\Big)^{\frac{\lambda_{\min}}{\ln\lambda_{\min}}}\Big) \triangleq \beta(\lambda_1,\lambda_2), && (21) \end{aligned}$$

where (20) follows from replacing n_0 using (17). Note that $\beta(\lambda_1,\lambda_2)$ as defined in (21) is not a function of n_0. Further, replacing $\frac{\lambda'-\lambda''}{\ln\lambda'-\ln\lambda''}$ with $\frac{\lambda_{\min}}{\ln\lambda_{\min}}$ in (21) allows $\beta(\lambda_1,\lambda_2)$ to be continuous and well behaved if $\lambda_1 \to \lambda_2$. We can now approximate (18) as

$$\begin{aligned} \Phi(\lambda_1,\lambda_2,n_0) \approx \max(\log p(n_0;\lambda_1), \log p(n_0;\lambda_2)) \\ - 1 + \beta(\lambda_1,\lambda_2), \end{aligned} \quad (22)$$

The entropy of the Poisson mixture in (12) can then be

approximated using (22) as

$$
\begin{aligned}
&H(Y)\\
&\approx -\frac{1}{2}\sum_n \Big(p(n;\lambda_1)+p(n;\lambda_2)\Big)\\
&\quad\cdot\Big[\max(\log p(n;\lambda_1),\log p(n;\lambda_2))-1+\beta(\lambda_1,\lambda_2)\Big] \quad (23)\\
&=-\frac{1}{2}\sum_n p(n;\lambda_1)\max(\log p(n;\lambda_1),\log p(n;\lambda_2))\\
&\quad-\frac{1}{2}\sum_n p(n;\lambda_2)\max(\log p(n;\lambda_1),\log p(n;\lambda_2))\\
&\quad+1-\beta(\lambda_1,\lambda_2) \quad (24)\\
&\le -\frac{1}{2}\sum_n p(n;\lambda_1)\log p(n;\lambda_1)-\frac{1}{2}\sum_n p(n;\lambda_2)\log p(n;\lambda_2))\\
&\quad+1-\beta(\lambda_1,\lambda_2) \quad (25)\\
&=\frac{1}{2}H(N_{\lambda_1})+\frac{1}{2}H(N_{\lambda_2})+1-\beta(\lambda_1,\lambda_2)\text{ bits}, \quad (26)
\end{aligned}
$$

where in (24) we have used the property $\sum_n p(n;\lambda_i)=1$, and in (25) we used the following inequality:

$$\log p(n;\lambda_i)\le \max(\log p(n;\lambda_1),\log p(n;\lambda_2))\,,\ i=1,2.$$

Fig. 2 shows the approximation obtained using (26) compared to the true entropy (12) over a sample range of λ's. The "true" entropy values for $H(N_{\lambda_1}), H(N_{\lambda_2})$ are estimated using numerical calculations. We observe that the derived closed-form expression provides a simple, effective approximation for the entropy of a Poisson mixture. As the ratio $(\lambda_{\text{min}}/\lambda_{\text{max}})$ decreases, the approximation serves as an excellent estimate of the entropy function. The approximation also equals the entropy when $\lambda_1=\lambda_2$.

B. Approximating MI over the SER channel

The MI between two random variables X and Y is given by

$$I(X;Y)=H(Y)-H(Y|X). \quad (27)$$

Using (9), (26) and (27), we obtain a corresponding approximation for the MI over the SER channel as

$$I(X;Y)\approx 1-\beta(\lambda_1,\lambda_2)\text{ bits}. \quad (28)$$

We observe that the analytical expression in (28) no longer requires the estimation of entropy of the individual Poisson distributions. Further, the expression is no longer a function of n, and has a constant order of complexity, thus leading to a significant speed up when evaluating this expression. Fig. 3 shows approximation for a large range of values for the pair (λ_1,λ_2). Since X is drawn from an equiprobable Bernoulli the MI is upper bounded as $I(X;Y)\le H(X)=1$ bit.

IV. Results and Discussion

Here, the input X to the SER channel is determined by both the frequency and intensity of the stimulus tone as defined in (5). The corresponding mean spike rate in response to the input is then estimated by pooling multi-unit data of the selected

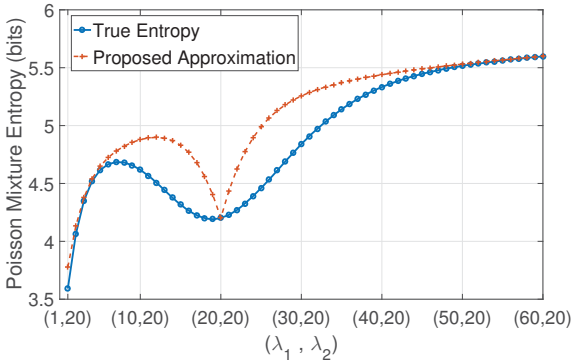

Fig. 2: Approximating the entropy of the Poisson mixture. The value of λ_1 is varied while λ_2 is kept constant.

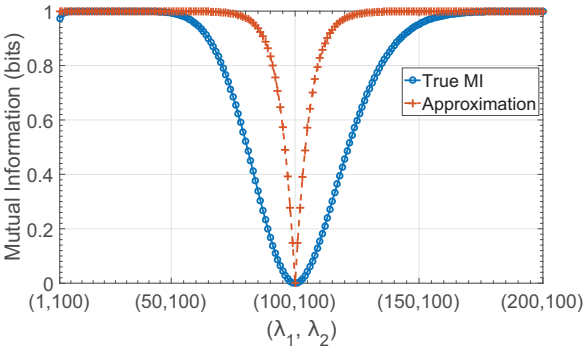

Fig. 3: Approximating the MI over the SER channel. The value of λ_1 is varied while λ_2 is kept constant.

stimulus tone across all recording depths and repetitions. The MI over the SER channel is then estimated using (28).

Table. I lists the MI estimates for each of the seven electrodes, wherein the input realization x_1 corresponds to a high relevance tone of frequency 1 kHz, and intensity 53 dB SPL. The MI estimates are averaged across all electrodes to obtain a mean mutual information $\overline{\text{MI}}$. Fig. 4(a) shows the $\overline{\text{MI}}$ calculated for tones of high relevance frequency 1 kHz, as a function of sound intensity. The MI estimate of the population response increases with increasing sound intensity, as expected based on overall increased firing rate with increased sound intensity.

Alternatively, in Fig. 4(b) we calculate the $\overline{\text{MI}}$ for tones of all frequencies, collapsed across sound intensity. In other words, all tones of a given frequency are considered realizations of x_1 regardless of their intensity, and the mean spike rate is estimated by pooling data across repetitions of that same frequency, i.e., across all four sound intensities. Comparing the high relevance frequency versus low relevance frequencies in Fig. 4(b), our analysis reveals MI tuning to the high relevance frequency, observed as a notch in Fig. 4(b). These findings suggest that the operating range of the auditory cortex can adapt to the behavioral relevance of auditory stimuli, at least when using population coding.

In summary, here we have proposed and applied a new information theoretic model to quantify changes in neuronal discharge patterns in response to stimuli of different behav-

ioral relevance. Results hint that MI decreases for highly behaviorally relevant sound, consistent with a potential change from neuronal rate to temporal code for highly relevant sound. This suggests that the proposed approach is a useful tool for quantifying neuronal responses.

TABLE I: Spike rates and MI estimates over the SER channel for the input tone of 1 kHz at 53 dB SPL. Averaging over all electrodes, $\overline{\text{MI}} = 0.806$.

Electrode	1 kHz, 53 dB, λ_1	Silence, λ_2	MI estimates
5	22	20	0.387
6	211	154	0.999
7	168	142	0.988
13	18	15	0.552
14	51	44	0.761
15	52	36	0.964
16	227	198	0.991

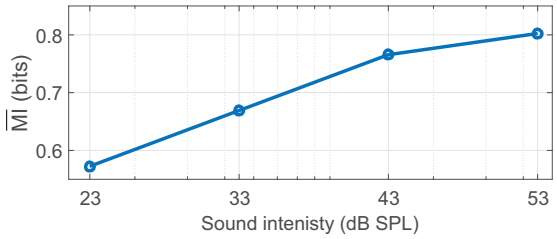

(a) Response to high relevance frequency 1 kHz

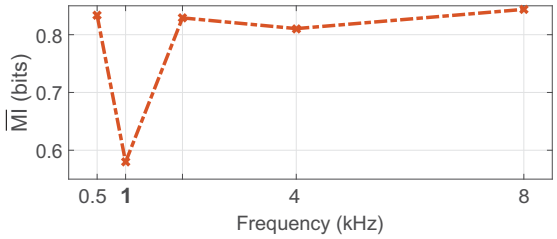

(b) Response for **high** versus low relevance frequencies

Fig. 4: Estimated MI over the SER channel. (a) MI estimates for tones of high relevance frequency 1 kHz, as a function of sound intensity. (b) MI estimates for high relevance frequency versus low relevance frequencies, pooled across all four sound intensities for each given frequency.

REFERENCES

[1] M. N. Shadlen and W. T. Newsome, "Noise, neural codes and cortical organization," *Current Opinion in Neurobiology*, vol. 4, no. 4, pp. 569–579, 1994.

[2] C. F. Stevens and A. M. Zador, "Information through a spiking neuron," in *Advances in Neural Information Processing Systems*, 1996, pp. 75–81.

[3] F. Rieke, D. Warland, R. De Ruyter van Steveninck, and W. Bialek, *Spikes: Exploring the Neural Code*. The MIT Press, 1999.

[4] A. Borst and F. E. Theunissen, "Information theory and neural coding," *Nature Neuroscience*, vol. 2, no. 11, pp. 947–957, 1999.

[5] A. G. Dimitrov, A. A. Lazar, and J. D. Victor, "Information theory in neuroscience," *Journal of Computational Neuroscience*, vol. 30, no. 1, pp. 1–5, 2011.

[6] S. Strong, R. D. R. Van Steveninck, W. Bialek, and R. Koberle, "On the application of information theory to neural spike trains," in *Pac Symp Biocomput*, vol. 1998, 1998, pp. 621–632.

[7] K. Wimmer, K. J. Hildebrandt, R. M. Hennig, and K. Obermayer, "Adaptation and selective information transmission in the cricket auditory neuron an2," *PLoS Computational Biology*, vol. 4, no. 9, p. e1000182, 2008.

[8] M. Pachitariu, D. R. Lyamzin, M. Sahani, and N. A. Lesica, "State-dependent population coding in primary auditory cortex," *Journal of Neuroscience*, vol. 35, no. 5, pp. 2058–2073, 2015.

[9] S. Panzeri and S. R. Schultz, "A unified approach to the study of temporal, correlational, and rate coding," *Neural Computation*, vol. 13, no. 6, pp. 1311–1349, 2001.

[10] S. Panzeri, R. S. Petersen, S. R. Schultz, M. Lebedev, and M. E. Diamond, "The role of spike timing in the coding of stimulus location in rat somatosensory cortex," *Neuron*, vol. 29, no. 3, pp. 769–777, 2001.

[11] E. T. Rolls, H. D. Critchley, and A. Treves, "Representation of olfactory information in the primate orbitofrontal cortex," *Journal of Neurophysiology*, vol. 75, no. 5, pp. 1982–1996, 1996.

[12] S. Jaramillo and A. M. Zador, "The auditory cortex mediates the perceptual effects of acoustic temporal expectation," *Nature Neuroscience*, vol. 14, no. 2, p. 246, 2011.

[13] M. S. Osmanski and X. Wang, "Behavioral dependence of auditory cortical responses," *Brain Topography*, vol. 28, no. 3, pp. 365–378, 2015.

[14] S. V. David, "Incorporating behavioral and sensory context into spectro-temporal models of auditory encoding," *Hearing Research*, 2017.

[15] J. J. Eggermont, "Between sound and perception: reviewing the search for a neural code," *Hearing Research*, vol. 157, no. 1, pp. 1–42, 2001.

[16] C. Micheyl, P. R. Schrater, and A. J. Oxenham, "Auditory frequency and intensity discrimination explained using a cortical population rate code," *PLoS Computational Biology*, vol. 9, no. 11, p. e1003336, 2013.

[17] C. Kayser, N. K. Logothetis, and S. Panzeri, "Millisecond encoding precision of auditory cortex neurons," *Proceedings of the National Academy of Sciences*, vol. 107, no. 39, pp. 16 976–16 981, 2010.

[18] K. M. Walker, J. K. Bizley, A. J. King, and J. W. Schnupp, "Cortical encoding of pitch: recent results and open questions," *Hearing Research*, vol. 271, no. 1, pp. 74–87, 2011.

[19] M. R. DeWeese and A. M. Zador, "Binary coding in auditory cortex," in *Advances in Neural Information Processing Systems*, 2003, pp. 117–124.

[20] M. C. Wiener and B. J. Richmond, "Decoding spike trains instant by instant using order statistics and the mixture-of-poissons model," *Journal of Neuroscience*, vol. 23, no. 6, pp. 2394–2406, 2003.

[21] S. W. Linderman, M. J. Johnson, M. A. Wilson, and Z. Chen, "A nonparametric bayesian approach for uncovering rat hippocampal population codes during spatial navigation," *Journal of Neuroscience Methods*, vol. 263, p. 36, 2016.

[22] J. A. Adell, A. Lekuona *et al.*, "Sharp estimates in signed poisson approximation of poisson mixtures," *Bernoulli*, vol. 11, no. 1, pp. 47–65, 2005.

[23] B. Roos, "Improvements in the poisson approximation of mixed poisson distributions," *Journal of Statistical Planning and Inference*, vol. 113, no. 2, pp. 467–483, 2003.

[24] M. Kittel, E. Wagner, and G. M. Klump, "An estimate of the auditory-filter bandwidth in the Mongolian Gerbil," *Hearing Research*, vol. 164, no. 1, pp. 69–76, 2002.

[25] O. Gleich, M. C. Kittel, G. M. Klump, and J. Strutz, "Temporal integration in the gerbil: the effects of age, hearing loss and temporally unmodulated and modulated speech-like masker noises," *Hearing Research*, vol. 224, no. 1, pp. 101–114, 2007.

[26] G. von Trapp, B. N. Buran, K. Sen, M. N. Semple, and D. H. Sanes, "A decline in response variability improves neural signal detection during auditory task performance," *Journal of Neuroscience*, vol. 36, no. 43, pp. 11 097–11 106, 2016.

[27] A. Ihlefeld, Y.-W. Chen, and D. H. Sanes, "Developmental conductive hearing loss reduces modulation masking release," *Trends in Hearing*, vol. 20, p. 2331216516676255, 2016.

[28] H. G. Rey, C. Pedreira, and R. Q. Quiroga, "Past, present and future of spike sorting techniques," *Brain Research Bulletin*, vol. 119, pp. 106–117, 2015.

[29] R. Q. Quiroga, Z. Nadasdy, and Y. Ben-Shaul, "Unsupervised spike detection and sorting with wavelets and superparamagnetic clustering," *Neural computation*, vol. 16, no. 8, pp. 1661–1687, 2004.

[30] W. Feller, *An Introduction to Probability Theory and Its Applications*. John Wiley & Sons, 2008, vol. 2.

[31] P. B. Borwein, "On the complexity of calculating factorials," *Journal of Algorithms*, vol. 6, no. 3, pp. 376–380, 1985.